

USING X-RAY SCATTERING TO CHARACTERIZE THE NANOSTRUCTURES OF DOT ARRAYS

Nanodot systems (periodic arrays of nanostructured dots) are drawing great interest for their potential use in future high-density optical and magnetic media storage devices. Researchers at the APS have demonstrated that x-ray scattering can be used to precisely characterize these deep nanostructures to a degree of accuracy that has been unattainable with microscopy techniques.

The novel electrical, magnetic, and photonic properties of nanodot systems are based on their structural parameters. Quantitative analysis of an x-ray diffraction pattern from a mesoscopic two-dimensional array of nanofabricated dots is challenging because its reciprocal space density is many orders of magnitude higher than those of typical solid-state or biological crystals.

Researchers from Argonne National Laboratory; The University of California, San Diego, Los Alamos National Laboratory, the University of Illinois at Chicago; and Cornell University have overcome that challenge: they found that the diffraction pattern exhibits characteristic features because of the highly anisotropic nature of the instrumental resolution function, which can be understood as analogs of Kossel lines—or pseudo-Kossel lines. Although such an unusual diffraction pattern had already been observed [1], researchers at the APS have gone beyond previous research to explain this unique pattern by using a clear, simple resolution function.

The sample for analysis was prepared by using a standard lithography and lift-off process to fabricate a square array of circular disk-shaped dots with a period of 750 nm and a diameter of 340 nm. E-beam lithography was used to prepare the required pattern in a single poly(methyl-methacrylate) layer, and e-beam evaporation was used to deposit a 50-nm-thick Gd film. An area of $0.5 \times 0.5 \text{ mm}^2$ was patterned on a $10 \times 10\text{-mm}^2$ Si/SiO₂ wafer. Researchers then took x-ray diffraction measurements using 9-keV monochromatic x-rays at the XOR beamlines 1-BM, 2-BM, and 4-ID-D at the APS. In contrast to scanning electron microscopy (SEM) or atomic force microscopy (AFM)—which are highly effective microscopy tools for topical measurements—the primary benefit of x-ray scattering is that the measurements take the structural average of the entire sample.

By using their technique, researchers can characterize the “deep” nanostructures that can be difficult to characterize by using SEM or AFM (Fig. 1). Moreover, once researchers combined their technique and analysis concept with magnetization-sensitive x-ray or neutron measurements, they found that the diffraction measurements from the mesoscopic magnetic dot (or pattern) arrays could be explained without a failure, and excellent results were finally obtained [2, 3].

The research at the APS demonstrates that x-ray scattering augments the capabilities of SEM and AFM, since it can be used to characterize the structural details of deep nanostructures and measure the buried interfaces. Ultimately, the work at the APS may help to advance nanofabrication technology. ○

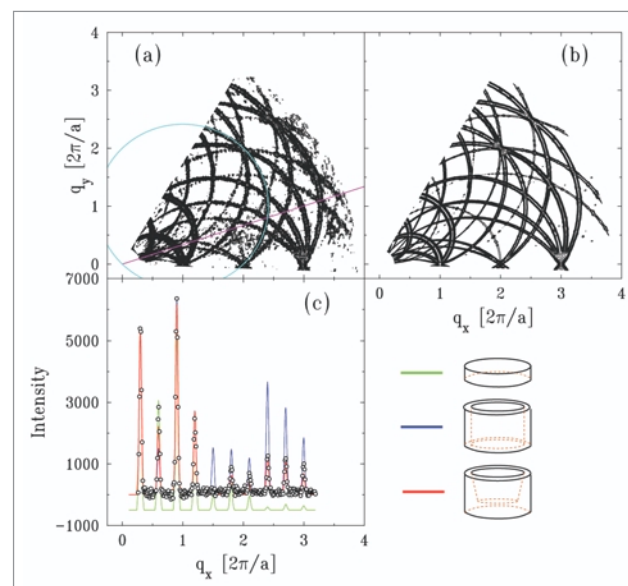


Fig. 1. Contour map of intensity distribution in the q_x - q_y reciprocal plane: (a) measurements and (b) calculations with horizontal resolution width of $2.75 \times 10^{-3} \text{ \AA}^{-1}$. For reference, $2\pi/a$ corresponds to $8.37 \times 10^{-4} \text{ \AA}^{-1}$. The circle in (a) shows a pseudo-Kossel circle. Pseudo-Kossel lines, like real Kossel lines in crystalline samples, can be used for precise characterization of the nanostructures of the dot array. (c) Diffraction intensities of the radial scan along the (3 1) direction, the trajectory of which is indicated by the line in (a). Circles represent measurements, and lines represent the calculations with different models: circular disks (green), ring cylinders (blue), and crowns (red), as shown in the inset. For clarity, the green line is shifted.

References

- [1] D. Rafaja, V. Valvoda, J. Kub, K. Temst, M.J. Van Bael, and Y. Bruynseraede, *Phys. Rev. B* **61**, 16144 (2000).
- [2] D.R. Lee, G. Srajer, M.R. Fitzsimmons, V. Metlushko, and S. K. Sinha, *Appl. Phys. Lett.* **82**(1), 82 (2003).
- [3] D.R. Lee, J.W. Freeland, G. Srajer, S.K. Sinha, V. Metlushko, and B. Ilıc, submitted to *Phys. Rev. B*; (available at <http://xxx.lanl.gov/abs/cond-mat/0309672>).

See: D.R. Lee¹, Y.S. Chu¹, Y. Choi¹, J.C. Lang¹, G. Srajer¹, S.K. Sinha², V. Metlushko³, and B. Ilıc⁴, “Characterization of the nanostructures of a lithographically patterned dot array by x-ray pseudo-Kossel lines,” *Appl. Phys. Lett.* **82**(6), 982-984 (10 February 2003).

Author affiliations: ¹Argonne National Laboratory, ²University of California, San Diego, and Los Alamos National Laboratory, ³University of Illinois at Chicago, ⁴Cornell University

V.M. is supported by NSF Grant No. ECS-0202780. S.K.S. is supported by the U.S. Department of Energy (DOE), Office of Science, Office of Basic Energy Sciences (BES)-Materials Sciences and Engineering Division under contract No. W-7405-Eng-36. Use of the APS supported by the U.S. DOE, Office of Science, BES, under Contract No. W-31-109-Eng-38.

EVALUATING THE FORCED OXIDATION OF FERROMAGNETIC CONTACTS IN MAGNETIC TUNNEL JUNCTIONS

Magnetic tunnel junction (MTJ) devices are broadly used because of the ability to attain high values of tunneling magnetoresistance (TMR). However, the role of interface structure is key to the performance of these devices. To understand this issue, researchers need to determine how best to form a high-quality insulating oxide spacer without influencing the quality of neighboring ferromagnetic contacts. At the APS, researchers studied forced oxidation of ferromagnetic contacts in magnetic tunnel junctions. As a result of their research, they concluded that microstructure plays an important role in determining the impact of the oxidation process on the layers.

Experiments were performed at XOR sector 4 of the APS by using the intermediate energy beam line (4-ID-C). Researchers used samples consisting of an MTJ with a wedge-shaped Al oxide-insulating layer. The full structure was $\text{SiO}_2/\text{IrMn}/\text{CoFe}$ (30 Å)/ Al_2O_3 (x Å)/ NiFeCo (30 Å), where x ranges from 5–20 Å. Polarization-dependent X-ray absorption and scattering—which is element-selective and therefore layer-selective—was used to provide detailed information about the chemical and magnetic state of the separate layers.

Although the absorption provides insight into a large portion of the CoFe layer, the TMR is still strongly sensitive to the oxidation at the $\text{Al}_2\text{O}_3/\text{CoFe}$ interface. By using x-ray reflectivity at the Co L_3 resonance, which is sensitive to the top 2–3 Å of CoFe, researchers can directly probe the chemical state at the boundary. If the oxide is present first in the grain boundary, it will show clearly in the absorption. However, the grain boundary comprises a small fraction of the interface, and so the interface signal will be dominated by the Al_2O_3 /metal CoFe signature. This is also consistent with nonzero MR in the overoxidized region. Until the aluminum thickness is reduced to around 6 Å, there are still regions of metallic CoFe in contact with Al_2O_3 . The MR decreases in this region because the density/area of metal/ Al_2O_3 is decreasing.

Another major issue to address is the change in the structure after annealing in applied field to 200°C, which is required for attaining the highest TMR values. Are changes in the magnetic response due to structural or magnetic changes? Measurements of the x-ray resonant diffuse scattering allow the chemical and magnetic interface structure to be determined in a layer-by-layer fashion. Scattering at the Mn, Co, and Ni L_3 edges provides element- (and, therefore, layer-) specific information. Figure 1 shows a set of rocking curves measured at the Mn and Ni L edges. By analyzing the rocking curves, researchers found that the preanneal structure is characterized

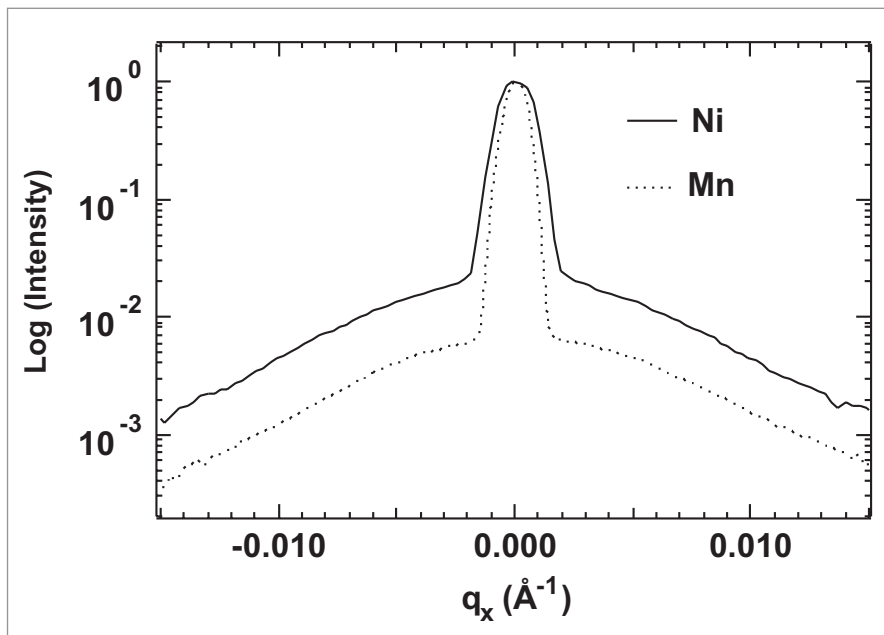


Fig. 1. X-ray resonant rocking curves at the Ni and Mn L_3 edges measured after field annealing.

by a conformal roughness (perpendicular roughness = 3 Å and in-plane roughness = 300 Å) propagating through the whole structure. After the anneal, there is no change, indicating that the structure is stable under these conditions and all magnetic changes are due solely to dipolar fields from the alignment of the random domains on the IrMn exchange bias layer. This finding confirms that the origin of changes in the TMR must be magnetic, not structural.

Overoxidizing the layers of a magnetic tunnel junction provided new insights into the impact of unwanted oxidation. APS researchers concluded that, from the evidence of grain boundary diffusion, the microstructure plays an important role in determining the impact of the oxidation process. From the perspective of TMR, they found that the main contribution to the change with field annealing appeared to be due to change in the layer-dependent switching after field annealing. ○

See: J.W. Freeland¹, D.J. Keavney¹, R. Winarski¹, P. Ryan¹, J.M. Slaughter², R.W. Dave², and J. Janesky², "Grain boundary mediated oxidation and interlayer dipolar coupling in a magnetic tunnel junction structure," *Phys. Rev. B* **67**, 134411-1 to 143311-4 (17 January 2003).

Author affiliations: ¹Argonne National Laboratory, ²Motorola Labs

Work at Motorola Labs was supported in part by DARPA. Use of the Advanced Photon Source was supported by the U.S. Department of Energy, Office of Science, Office of Basic Energy Sciences, under Contract No. W-31-109-Eng-38.

NEW INFORMATION ON MAGNETIC SEMICONDUCTORS

Manipulation of electron spin, as well as charge, in electronic devices may allow researchers to examine and control spin under very well controlled environments and to develop new functions in future magnetic semiconductor-based devices. A key question is resolving the details of the electronic structure and the origin of the states that participate in the magnetic coupling. To fully realize the potential of this technology, APS researchers sought to fully understand the origin of ferromagnetic ordering in Mn-doped GaAs. By using x-ray magnetic circular dichroism at the Mn, Ga, and As $L_{3,2}$ edges, researchers using the XOR 4-ID-C soft x-ray beamline at the APS have detected induced Ga and As moments in ferromagnetic $\text{Ga}_{1-x}\text{Mn}_x\text{As}$.

Mn-doped GaAs is ideal for exploring the origins of ferromagnetic ordering in this class of materials. Polarized holes that are primarily derived from As 4p valence band states are generally thought to mediate the coupling between Mn. Recent calculations of the band structure for Mn-doped GaAs predict an induced magnetic moment on the As atoms that is antiparallel to the Mn 3d moments and a smaller parallel Ga moment. Soft x-ray magnetic circular dichroism (XMCD) provides element-specific magnetic information, so it is a powerful technique to test for the presence of these moments.

APS researchers found an As magnetic moment antiparallel to the Mn and a very small parallel Ga moment by using XMCD at the Mn, Ga, and As $L_{3,2}$ edges in molecular beam epitaxy (MBE)-grown films of $\text{Ga}_{1-x}\text{Mn}_x\text{As}$ (with $x = 0.039, 0.049, 0.059, 0.07, \text{ and } 0.081$). The 4-ID-C soft x-ray beamline was used to make the XMCD measurements. Researchers used total electron yield to measure x-ray absorption and dichroism. Dichroism scans were taken at fixed photon polarization by reversing the magnetization of the sample at each energy.

Figure 1 shows a plot of the Mn, Ga, and As L edge dichroism taken from the $x = 0.07$ sample. As shown in the figure, both the As and Ga L_3 data display a weak dichroism at the onset of the absorption edge jump, indicating a magnetic moment on each. By applying selection rules to these transitions, researchers determined that the orientations of the induced host moments are antiparallel to the Mn for As and parallel for Ga. Figure 2 shows the field and temperature dependence of the Ga and Mn signals. This figure shows that the Ga dichroism signal follows very closely that of the Mn and is clearly associated with the ordering of the Mn. These results are consistent with the notion that polarized As valence band holes mediate the ferromagnetic coupling between Mn ions in $\text{Ga}_{1-x}\text{Mn}_x\text{As}$. By comparing the areas under the As and Ga L_3 dichroism curves, researchers obtained an estimate of the relative sizes of the As and Ga s spin moment per hole.

By using soft x-ray magnetic circular dichroism, APS researchers detected induced moments on both Ga and As in the ferromagnetic semiconductor $\text{Ga}_{1-x}\text{Mn}_x\text{As}$ and determined the relative spin orientations of each atomic species. They found, for example, that the As average moment is aligned antiparallel to that of the Mn, while the Ga is parallel. The results show that the hole states that mediate the ferromagnetic ordering are derived primarily from As, and that these As valence band states are antiferromagnetically coupled to the Mn 3d moments.

These results support the hole-mediated model of coupling in magnetic semiconductors and identify the electronic states that are involved. This investigation will help other researchers design new materials with enhanced magnetic properties. A principal goal is a room-temperature

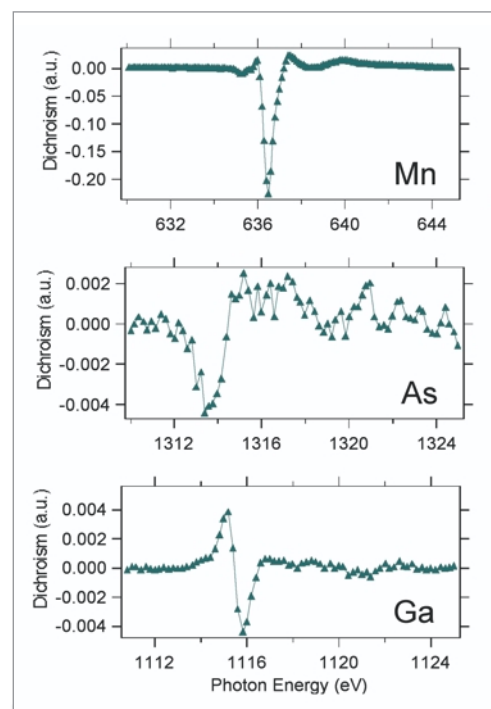


Fig. 1. X-ray magnetic circular dichroism observed at the Mn, As, and Ga L_3 edges for the $x = 0.07$ sample.

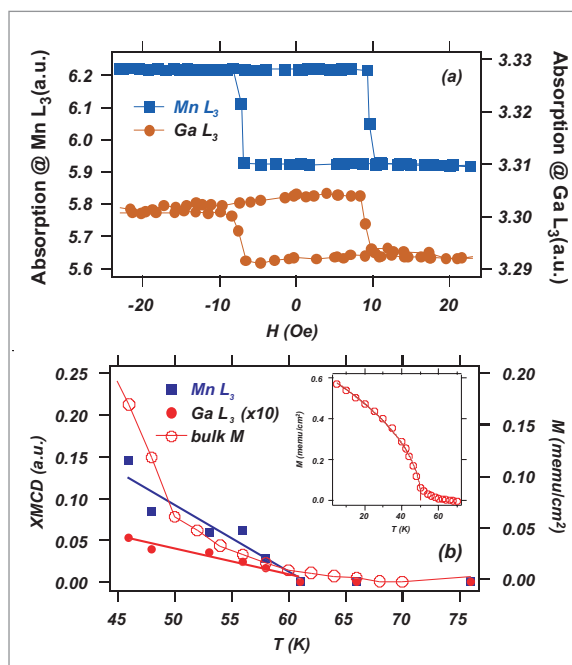


Fig. 2. Magnetic field (a) and temperature (b) dependence of the dichroism signals seen at the Mn and Ga L edges for $x = 0.049$. Field dependence data were taken at 44K, and temperature dependence at zero field. Inset in (b) shows bulk magnetization (M) data for the same sample.

magnetic semiconductor that is compatible with the existing semiconductor fabrication technology, which is important for the realization of spin-based devices. Researchers are now using the APS to examine similar issues in other Mn-doped semiconductors, such as GaN and InAs. Further experiments are planned on $\text{Ga}_{1-x}\text{Mn}_x\text{As}$ to examine in greater detail the locations of the Mn ions within the GaAs lattice. ○

See: D.J. Keavney¹, D. Wu², J.W. Freeland¹, E. Johnston-Halperin³, D.D. Awschalom³, and J. Shi², "Element Resolved Spin Configuration in Ferromagnetic Manganese-Doped

Gallium Arsenide," *Phys. Rev. Lett.* **91**(18), 187203-1 to 187203-4 (31 October 2003).

Author affiliations: ¹Argonne National Laboratory, ²University of Utah, ³University of California, Santa Barbara

Work at the University of Utah was supported by the ONR/DARPA under Grant No. N00014-02-10595, and at UCSB by ONR/DARPA under Grant No. N00014-99-1-1096 and AFOSR F49620-02-10036. Use of the Advanced Photon Source was supported by the U.S. Department of Energy, Office of Science, Office of Basic Energy Sciences, under Contract No. W-31-109-Eng-38.

A QUANTITATIVE PICTURE OF STRAIN GENERATION DUE TO DENSE ELECTRON-HOLE PLASMAS

Researchers from the University of Michigan; the University of California, Berkeley; Kansas State University; the University of Oxford; and University College in Cork, Ireland, are pioneering a new technique for studying strain generation and propagation in crystalline solids. The APS's high-brightness, short-pulse, hard x-rays permit probing of coherent strain generation and propagation in both the frequency and time domains through the use of time-resolved x-ray anomalous transmission, which, unlike other methods, can provide quantitative structural information.

X-rays establish two standing waves upon propagating along a particular direction through a periodic medium. These consist of an anomalous transmission wave (α -wave), which is minimally absorbed, and a β -wave, which is strongly absorbed. In thick crystals, the β -wave is absorbed almost completely, so what exits the crystal is mainly the anomalous wave, which propagates as two x-ray beams, one in the direction of the incident beam and the other in a deflected direction. The researchers have shown that a short acoustic pulse directed at the x-ray exit face of the crystal can coherently transfer energy between the α and β beams. Following an initial transient, the diffracted x-ray intensities oscillate in time as the pulse travels into the crystal. The relative phase of the oscillations and the amplitude of the transient provide information about the strain generation process at times shorter than the duration of the x-ray probe.

The researchers recently used the new technique as a bulk-sensitive structural probe in studying the propagation and lattice coupling of dense electron-hole plasmas produced by a subpicosecond laser. The experiments were performed at the MHATT/XOR 7-ID beamline, where the x-ray energy was set to 10 keV using a cryogenically cooled Si(111) double-crystal monochromator. Coherent strain pulses were produced on the x-ray exit face of a 280- μm thick germanium (Ge) single crystal by sub-100-fs, 800-nm laser pulses focused to a 1.5 mm^2 spot on the crystal surface. A fast silicon avalanche photodiode (APD) and a picosecond x-ray streak camera were used as the time-resolved detectors of the two exiting x-ray beams; the APD sampled the deflected-diffracted beam intensity while the

streak camera sampled the forward-diffracted beam. X-ray bunch separation was about 152 ns, which is large enough to allow electronic gating and measurement of single x-ray pulses. This is critical for ultrafast experiments where the laser repetition rate is typically considerably less than that of the x-ray pulses.

Following laser excitation, high-contrast oscillations were observed in the time-resolved x-ray data over a large span of excitation densities. The transient behavior is due to a perturbation in the lattice that reached a depth of more than 1.5 μm within 40 ps. Conceptualizing the strain as a moving interface that couples the α and β waves, the researchers concluded that the excitation must initially propagate into the bulk at speeds greater than 37,000 m/s, which is more than seven times the longitudinal speed of sound. The results are consistent with a picture in which electron-phonon coupling modified by carrier diffusion is the dominant mechanism for energy transport in laser-excited Ge. This research can be extended to study how the elastic response of the material can modify the electronic transport properties of semiconductors. ○

See: M.F. DeCamp¹, D.A. Reis¹, A. Cavalieri¹, P.H. Bucksbaum¹, R. Clarke¹, R. Merlin¹, E.M. Dufresne¹, D.A. Arms¹, A.M. Lindenberg², A.G. MacPhee², Z. Chang³, B. Lings⁴, J.S. Wark⁴, and S. Fahy⁵, "Transient Strain Driven by a Dense Electron-Hole Plasma," *Phys. Rev. Lett.* **91**(16), 165502-1 to 165502-4 (17 October 2003).

Author affiliations: ¹University of Michigan, ²University of California, Berkeley, ³Kansas State University, ⁴University of Oxford, ⁵University College

This work was supported in part by the U.S. Department of Energy, Grants No. DE-FG02-03ER46023 and No. DE-FG02-00ER15031; by the AFOSR under Contract No. F49620-00-1-0328 through the MURI program, and from the NSF FOCUS physics frontier center. S. F. acknowledges the financial support of the Science Foundation Ireland. Use of the Advanced Photon Source was supported by the U.S. Department of Energy, Office of Science, Office of Basic Energy Sciences, under Contract No. W-31-109-Eng-38.

LOCAL STRUCTURE OF MAGNETORESISTIVE OXIDES

Manganese-based magnetoresistive oxides are receiving increased attention because they show promise in a wide variety of applications, particularly spin-based electronics, or “spintronics.” The properties of magnetoresistive oxides depend sensitively on the structure of the MnO_6 octahedral building blocks that make up the crystal lattice. A deeper understanding of local structure—often studied using pair distribution function (PDF) analysis or x-ray absorption fine structure (XAFS)—is important because in many alloys it often differs from the average crystal structure probed by x-ray or neutron diffraction. Such diffraction studies have shown that in LaMnO_3 , the four short and two long bonds of the MnO_6 octahedra exhibit a Jahn-Teller distortion that is removed by Sr doping ($\text{La}_{1-x}\text{Sr}_x\text{MnO}_3$). At an Sr composition of $x \sim 0.175$, no long-range Jahn-Teller distortion exists at room temperature in the average structure. Previous studies of the local MnO_6 structure used the PDF of $\text{La}_{1-x}\text{Sr}_x\text{MnO}_3$ (LMSO) as a function of x at 10K and near room temperature to show that the local MnO_6 structure does differ from the average structure. The lengths of both the short and long Mn-O bonds changed little until local distortion disappeared, possibly forming localized three-site polarons though additional work produced conflicting results.

Using data collected at the MR-CAT 10-ID beamline at the APS, investigators from the University of Notre Dame and Argonne National Laboratory provided a more detailed picture of local structure by measuring Mn K-edge XAFS at $T \approx 10\text{K}$ and room temperature (290K) for various alloy compositions in the region $x < 0.475$, thereby establishing the local MnO_6 structure as a function of x . They discovered some distortion in the metallic phase, where x varied between 0.175 and 0.3, but found the bond length-splitting to be substantially smaller than the PDF results and the local distortion of MnO_6 strongly correlated with the electronic phase diagram.

Samples for the Mn K-edge XAFS experiments were those previously used for La K-edge and Sr K-edge XAFS studies. The Mn K-edge XAFS spectra were measured at sample holder temperatures of $T \approx 10\text{K}$ and 290K in transmission mode at the MR-CAT beamline at the APS. Duplicate or triplicate measurement of each sample allowed a check on the repeatability and noise level of the spectra, and a Fourier transform was fit to a model built with theoretical scattering paths.

Several different fit methods were used to deal with parameter correlations among the Mn-O bond lengths, the Debye Waller Factor (DWF), and the population of short and long bonds. For example, the number of long bonds (N_L) and the DWF are strongly correlated. N_L was thus constrained according to four models among which N_L varied.

The first coordination shell carries six oxygen atoms with 8 La/Sr second neighbors and 6 third neighbors around Mn ions. A systematic edge-energy shift with Sr composition is consistent

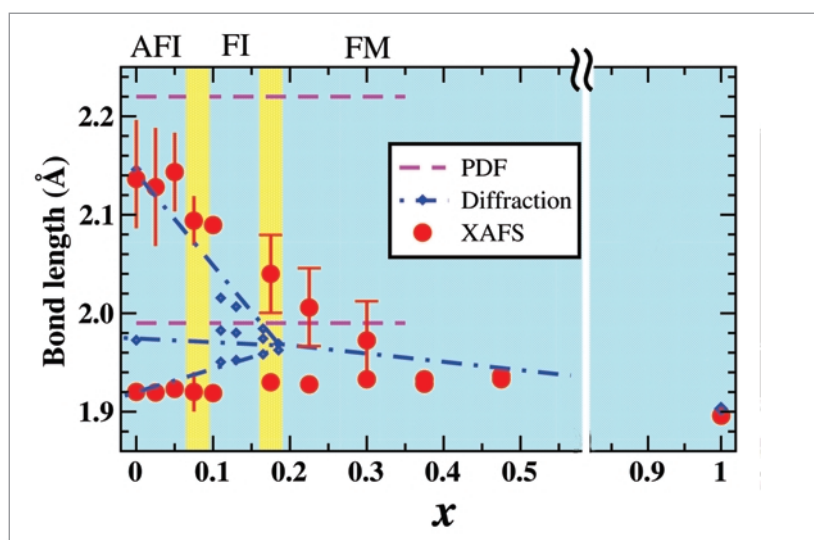


Fig. 1. Mn-O bond lengths as a function of x at 10K. Dots show low-temperature average structure from diffraction experiments. Hatched line is phase boundary: AFI (antiferromagnetic insulator), FI (ferromagnetic insulator), FM (ferromagnetic metal).

with the LSMO or other manganite systems, was observed. The long bond peak—a distinct feature for the LaMnO_3 —appears in samples with low Sr doping and shifts with doping for $x < 0.175$, nearly disappearing for $x > 0.175$ (Fig. 1). The largest deviation from the PDF results exists in the low- x region ($x < 0.35$). More detailed examination of these parameters shows either the absence of the bond at distances above 2.08 Å or a large length distribution, suggesting a maximum possible long bond length of about 2.08 Å , much shorter than that of LaMnO_3 (2.15 Å) or PDF results (2.22 Å). Room temperature results were similar to those at low temperature.

The finding that LaMnO_3 had three different bond lengths in average structure corroborates the previous PDF finding of three different bond lengths in local structure. The residual distortion found in the ferromagnetic metallic phase $x > 0.175$ is less than the PDF results. The XAFS results suggest that the structure does change with doping. Taken together, the data allow a detailed view of the Mn-O bonds. ○

See: T. Shibata¹, B.A. Bunker¹, and J.F. Mitchell², “Local distortion of MnO_6 clusters in the metallic phase of $\text{La}_{1-x}\text{Sr}_x\text{MnO}_3$,” *Phys. Rev. B* **68**, 024103-024112 (2003).

Author affiliations: ¹University of Notre Dame, ²Argonne National Laboratory

The MR-CAT is supported by the U.S. Department of Energy (DOE), DE-FG02-94-ER45525 and the member institutions. Use of the Advanced Photon Source was supported by the U.S. Department of Energy, Office of Science, Office of Basic Energy Sciences, under Contract No. W-31-109-Eng-38.

PROBING PICOSECOND DOMAIN DYNAMICS IN FERROELECTRICS BY USING SYNCHROTRON X-RAY BEAMS

Synchrotron x-rays open new doors for studying materials: researchers are now able to investigate much faster processes, analyze much weaker interactions among materials, and go much deeper into a material's interior—all at much better spatial resolution than before. In fact, the systematic use of synchrotron radiation for materials characterization has led to breakthroughs in many aspects of materials science. A good example is time-resolved x-ray diffraction measurements of very fast switching processes in ferroelectric thin films.

Researchers from the Technion-Israel Institute of Technology, and Northwestern University used the DND-CAT 5-BM-D beamline at the APS to carry out stroboscopic diffraction measurements with ferroelectric films subjected to strong periodic electric fields. The group found that the electric-field-induced variations of lattice parameters, as a function of delay time between the x-ray and electric signals, are well described by damped periodic functions, with the periodicity defined by the electric field frequency. They also found that the damping parameter is directly related to the system's attenuation time. They attribute the latter finding to the hindering of domain walls during domain switching as a result of their interaction with the arising deformation waves. This information may be important to the operation of devices based on ferroelectric films.

Ferroelectric materials have built-in electric dipoles, which produce net electric polarization without an external electric field (as magnetization in magnetic materials). Ferroelectric thin films are very promising for next-generation random access memories (RAM), since, in principle, these memory elements can be “trained” and used like in neural networks. As is the case for magnetic memories, the major factor that will determine the speed of future device operation will be the dynamics of ferroelectric domains in the ns to ps time scale. Today, researchers do not know how fast the ferroelectric memory could be and what the sources of limiting factors are. Complexity is increasing as domain size is reduced, which, in thin films, ranges from a few tens to a few hundreds of a nanometers. Probing fast-domain dynamics under an applied electric field in such nanostructures requires the development of novel experimental techniques.

The research at the APS is significant in that a novel experimental technique—stroboscopic x-ray diffraction on synchrotron beamlines—has now been used to characterize domain motion. This technique utilizes in-time synchronization between synchrotron x-ray bursts and periodic external field (in this case, an electric field) applied to the sample. In the stroboscopic mode of measurement, the phase difference between the periodic electric signal and the x-ray burst periodicity is kept constant during a single measurement run. After that, the

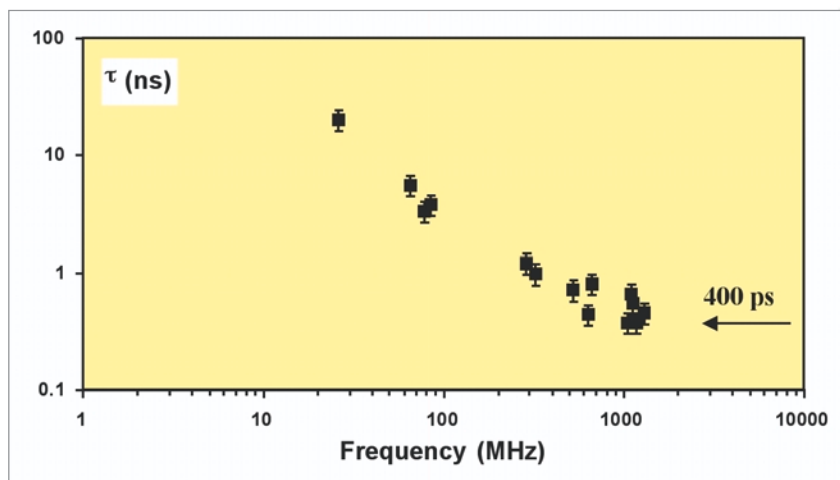


Fig. 1. Attenuation times, τ , of domain motions stroboscopically measured in a wide range of electric field frequencies between 25 MHz and 1.3 GHz.

phase shift is changed by means of a programmable delay unit, and measurements are continued. Changes in lattice parameters, measured as a function of the delay time, make domain dynamics “visible,” providing spectral characteristics of domain motion.

In this research, 200-nm-thick BaTiO_3 films, epitaxially grown on 500- μm -thick (100) MgO substrates, served as samples. Researchers used the stroboscopic registration of 25-keV x-rays diffracted from the ferroelectric films under an alternating current electric field with an amplitude of a few MV/m. For this purpose, electric pulses with a frequency of 6.517 MHz from a bunch clock generator of the APS storage ring were passed through a programmable delay unit (the minimal step was 18 ps) and applied to the input of a frequency synthesizer. The latter generated sinusoidal signals of multiple frequencies between 25 MHz and 1.3 GHz, which were phase-locked to the x-ray burst periodicity. After amplification, the sinusoidal signals were applied to the ferroelectric films via interdigital electrodes deposited on top of them.

The measured attenuation times revealed rapid reduction with the electric field frequency (see Fig. 1). Shorter attenuation time means heavier damping of domain motion. In these experiments, researchers were able to measure extremely short attenuation times (down to 400 ps), which demonstrates the capabilities of the developed technique. On the basis of the collected experimental data, researchers concluded that, despite heavy damping, ferroelectric domains in BaTiO_3 films can be effectively switched by the applied electric field at least up to 1.3 GHz.

Further experimental and theoretical studies of domain damping are required in order to clarify the particular mechanisms, which are responsible for the observed relationship between attenuation time and frequency. ○

See: E. Zolotoyabko¹, J.P. Quintana², D.J. Towner², B.H. Hoerman², and B.W. Wessels², "Nanosecond-Scale Domain Dynamics in BaTiO₃ Probed by Time-Resolved X-ray Diffraction," *Ferroelectrics* **290**, 115-124, (2003).

Author affiliations: ¹Technion-Israel Institute of Technology, ²Northwestern University

DND-CAT is supported by the E. I. DuPont de Nemours & Co., the Dow Chemical Company, the U.S. NSF through grants DMR-9304725 and the State of Illinois through the Department of Commerce and the Board of Higher Education grant IBHE HECA NWU 96. Additional financial support from NSF under grant DMR-0076077 and ECS-0123469. Use of the Advanced Photon Source was supported by the U.S. Department of Energy, Office of Science, Office of Basic Energy Sciences, under Contract No. W-31-109-Eng-38.

ROOM-TEMPERATURE FERROMAGNETIC SEMICONDUCTORS: A CLOSER LOOK AT A PROMISING CANDIDATE

Ferromagnetic semiconductors that remain magnetic at and above room temperature are critical to the development of spintronics. Co-doped TiO₂ anatase is an oxide semiconductor that exhibits ferromagnetism well above room temperature. The thermally robust ferromagnetism is thought to be mediated by electrons from oxygen vacancies, but the mechanism has been elusive. Knowledge of the local structure of the magnetic dopant is critical to determining whether the magnetism is caused by elemental Co nanocrystals, or whether Co is a magnetic dopant in the host lattice. The latter is a necessary but insufficient condition for the material being a magnetic semiconductor. Investigators from the Pacific Northwest National Laboratory (PNNL) in Richland, Washington, used the APS to produce data showing that Co-doped TiO₂ anatase has a structure favorable for ferromagnetic semiconductor formation.

Based on extensive previous research focused on the nucleation and growth of this material, the PNNL team used oxygen-plasma-assisted molecular beam epitaxy (OPAMBE) to grow epitaxial Co_xTi_{1-x}O₂ on LaAlO₃(001) to produce either semiconducting or insulating films. Co K-shell x-ray absorption spectra for two representative films were used to determine the local structure around the Co dopant. One film, grown under oxygen-rich conditions, was insulating and atomically flat. A second film, grown under slightly oxygen-poor conditions, was semiconducting, but consisted of two phases—a continuous epitaxial anatase phase with very little Co, and smaller epitaxial particles of Co-enriched anatase that formed on the surface of the continuous film.

Co K-shell x-ray absorption near-edge structure (XANES) and extended x-ray absorption fine structure (EXAFS) were measured at the APS using the PNC/XOR beamlines 20-ID and 20-BM.

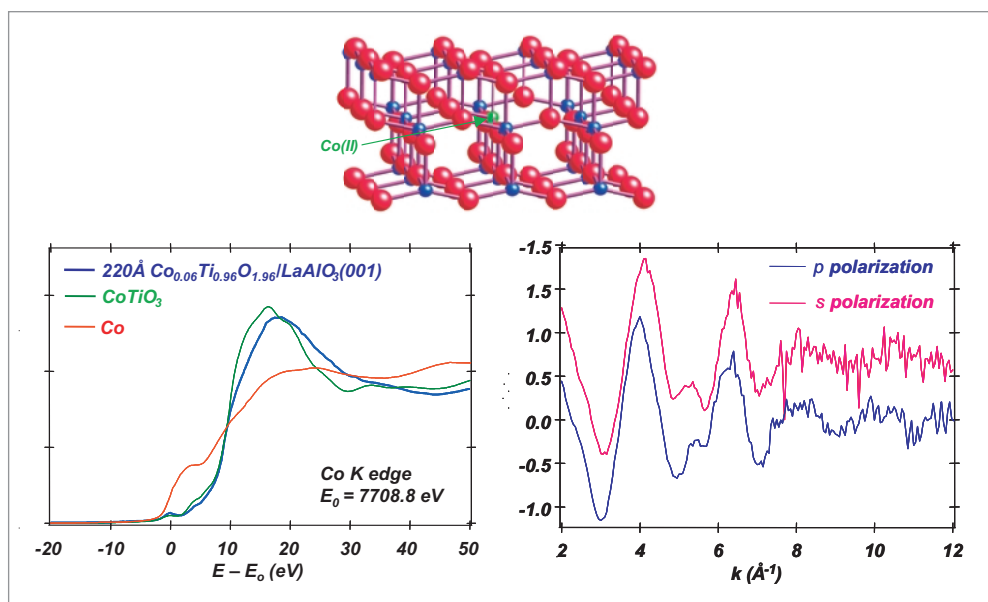


Fig. 1. Left: K-shell XANES for a 22-nm-thick Co_{0.06}Ti_{0.94}O_{1.94} epitaxial film on LaAlO₃(001) and appropriate standards. These spectra establish that the formal oxidation state of the Co is +2. Right: Co K-shell EXAFS for the same specimen in both s- and p-polarizations. The crystal model shows Co(II) substituting for Ti(IV) in the lattice, with an O vacancy adjacent to the Co(II). The O vacancy is required to maintain local charge neutrality.

The Co K-edge XANES (Fig. 1, left panel) are virtually identical for the two films and show that Co is in the +2 formal oxidation state. The spectra also reveal that the local structure resembles that of Co in CoTiO₃ more than CoO. There is no evidence for Co metal in either film. The Co K-edge is more sensitive to charge state and local structure than Co L-edge XANES, which was used in previous studies. Co L-edge XANES does not discriminate among Co, CoO, and CoTiO₃ as effectively.

Co K-shell EXAFS (Fig. 1, right panel) was used to determine the detailed structure of Co(II) in Co_xTi_{1-x}O₂. The two specimens exhibited similar oscillations and thus similar local structural environments for the Co. Fourier transforms and multiple scattering analyses for two x-ray polarizations showed bond lengths intermediate between those in pure anatase and the larger Co-O bond lengths in CoTiO₃, suggesting local strain fields at substitution sites. The Debye-Waller factors were also higher than expected for room-temperature Co-O bonds, presumably resulting from disorder at Co sites. The

spherically averaged effective coordination number was less than 6, indicating the presence of an oxygen vacancy in the vicinity of substitutional Co ions.

Expelling oxygen from the lattice produces strain relief and allows local charge neutrality to be maintained. Indeed, one O vacancy is required for each substitutional Co(II). The resulting empirical formula for Co-doped TiO_2 is $\text{Co}_x\text{Ti}_{1-x}\text{O}_{2-x}$. There is a significant but incomplete structural correlation between oxygen vacancies and substitutional Co(II). These oxygen vacancies do not, however, contribute to electrical conductivity, since the two electrons per vacancy are effectively bound to the nearby Co(II). In order to make the material semiconducting, oxygen vacancies greater than those needed to compensate substitutional Co(II) in $\text{Co}_x\text{Ti}_{1-x}\text{O}_{2-x}$ anatase are required.

These results establish that there is no detectable Co metal in OPAMBE-grown doped TiO_2 anatase. The magnetism is correlated with the presence of substitutional Co(II) in the anatase lattice and free carriers resulting from excess O vacancies. These results support, but do not prove, that Co-doped TiO_2 anatase is a true ferromagnetic semiconductor. Work on this and other magnetically doped oxide semiconductors is ongoing. ○

See: S.A. Chambers, S.M. Heald, and T. Droubay, "Local Co structure in epitaxial $\text{Co}_x\text{Ti}_{1-x}\text{O}_{2-x}$ anatase," *Phys. Rev. B* **67**, 100401-1 to 100401-4 (2003).

Author affiliation: Pacific Northwest National Laboratory

See also: S.A. Chambers and R.F.C. Farrow, "New Possibilities for Ferromagnetic Semiconductors," *MRS Bulletin* **28**, 729 (2003).

The film growth and *in situ* materials characterization described in this paper were performed in the Environmental Molecular Sciences Laboratory, a national scientific user facility sponsored by the DOE's Office of Biological and Environmental Research and located at PNNL. This work was supported by the PNNL Nanoscience and Technology Initiative, the U.S. DOE, Office of Science, Office of Basic Energy Sciences, Division of Materials Science, and the DARPA Spins in Semiconductors Initiative. The PNC/XOR is supported by funding from the U.S. DOE, Basic Energy Sciences, the NSF, the University of Washington, the Natural Sciences and Engineering Research Council in Canada, and Simon Fraser University. Use of the Advanced Photon Source was supported by the U.S. DOE, Office of Science, Office of Basic Energy Sciences, under Contract No. W-31-109-Eng-38.

FERROELECTRIC BONDING REVEALED BY X-RAY SCATTERING

Ferroelectric materials—substances that possess a permanent electric polarization—are of interest for a variety of potential technological applications, from sensors and displays to nonvolatile data storage. Although researchers have made significant progress in the theoretical understanding of these materials, some aspects of their behavior remain puzzling. In particular, the orbital symmetry of the bonds that are associated with the ferroelectric ordering has eluded detailed measurement. Recently, a team of researchers from the University of Pennsylvania and Argonne National Laboratory has used resonant x-ray scattering to observe the details of orbital ordering in a canonical ferroelectric, potassium niobate.

KNbO_3 was chosen for the present work in part because the nature of the niobium-oxygen bonds in this material is well understood and the computational results for the band structure are reliable. The ferroelectric properties of KNbO_3 arise from the highly directional bonding between the niobium and oxygen atoms (Fig. 1). Techniques such as x-ray absorption near-edge spectroscopy (XANES) have been used in the past to observe the directional bonding, but details of the orbital structure of these bonds are not revealed by these methods. Here, resonant x-ray scattering was used to observe the orbital symmetry in the ferroelectric ordering. Such studies could be extended to other materials, especially Pb- and Nb-based relaxor ferroelectrics.

A beam of polarized x-rays tuned near the niobium K edge at 18.987 keV is incident on a single crystal of KNbO_3 , which can be rotated to probe either the bonding or the nonbonding direction. Thermal diffuse x-ray scattering is collected near the Bragg peak positions with a solid-state detector, and these data

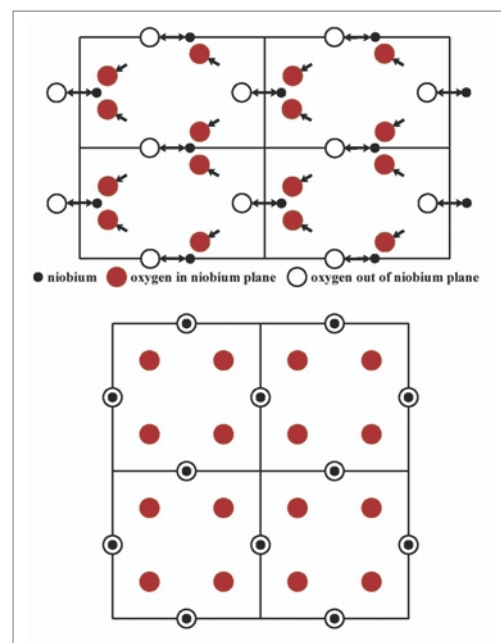


Fig. 1. The structure of niobium and oxygen in potassium niobate. At room temperature, KNbO_3 is orthorhombic (top), and displacement of the niobium and oxygen atoms produces a ferroelectric polarization. Above the Curie temperature, the structure is cubic and non-ferroelectric (bottom).

are used to construct x-ray dispersion curves. The anisotropy of the dispersion curves with respect to crystal orientation can be used to deduce the character of the niobium-oxygen bonds. Preliminary data were collected at beamline X25 at the National Synchrotron Light Source (NSLS), Brookhaven National

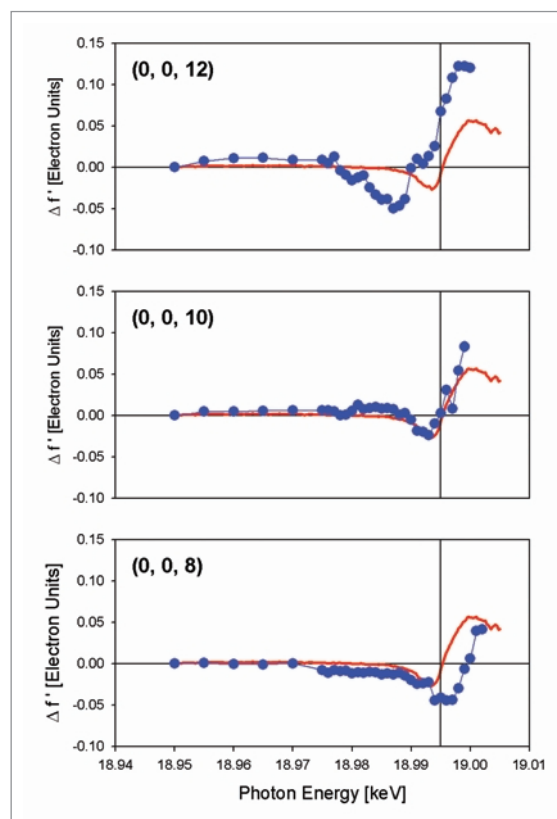
Fig. 2. Difference plots for the real part of the dispersion near the niobium K edge for three scattering momentum transfer vectors Q 's. The curves are obtained by subtracting the thermal diffuse scattering collected with x-ray polarization parallel to the lattice b axis from that collected with polarization parallel to the a axis (filled circles). Anisotropy of f' measured by XANES with no momentum resolution is shown as a solid line. The shift of the characteristic features toward lower energy with increasing Q is the result of increased involvement of d states in the bonding orbitals.

Laboratory, while the main set of experiments was carried out at the CMC-CAT beamline 9-ID at the APS.

From the collected data, difference plots of the anomalous dispersion curves are obtained that show the shifts in characteristic features as a function of Q , the momentum transfer vector (Fig. 2). Dipolar transitions involving states of p character are not dependent on Q , whereas the contribution of quadrupolar transition involving d states grows with increasing Q . Thus, the shift toward lower energy indicates that the lowest unoccupied states in the valence band probed by the resonant x-ray scattering are predominantly of d orbital symmetry.

The results show that resonant x-ray scattering can be a useful complement to XANES measurements in studying ferroelectric materials, particularly the details of the bonding that gives rise to their polarization properties. Moreover, given the subtlety of the shifts in anomalous dispersion, the high incident energy resolution offered by the monochromator crystals and third generation synchrotron at APS was essential in carrying out these experiments. Building on these results, the researchers now expect to be able to study even more complex ferroelectrics where the theoretical picture needs to be better understood. ○

See: E. Mamontov¹, T. Egami¹, W. Dmowski¹, T. Gog², and C. Venkataraman², "Anisotropic covalent bonds in KNbO_3 observed by resonant x-ray scattering," *Phys. Rev. B* **66**, 224105-1 to 224105-6 (10 December 2002).



© 2003 by The American Physical Society

Author affiliations: ¹University of Pennsylvania, ²CMC-CAT

The work at the University of Pennsylvania was supported by the Office of Naval Research through N000-14-01-10860. The NSLS is supported by the U.S. Department of Energy (DOE) Contract No. DE-AC02-98CH10866. Use of the Advanced Photon Source was supported by the DOE Office of Science, Office of Basic Energy Sciences, under Contract No. W-31-109-Eng-38.

UNUSUAL TOPOLOGICAL CHARGE FLUCTUATIONS IN AN ANTIFERROMAGNETIC COPPER OXIDE MATERIAL

High-temperature superconductivity in cuprate materials, colossal magnetoresistance in the manganates, and unusually intense nonlinear optical response in nickelates are all phenomena thought to result from very strong interactions among electrons in these materials. According to theory, some of these compounds should also exhibit other unusual physical properties, such as the separation of charge and spin fluctuations in the form of exotic quanta called holons and spinons. Researchers have been turning to inelastic x-ray scattering as a way of probing the details of electronic structure. Recently, a team of researchers from Princeton University, Argonne National Laboratory, Lawrence Berkeley National Laboratory, the Nano-electronic Research Center in Tsukuba, Japan, and the University of Tokyo used resonant x-ray scattering to obtain direct evidence of holons in a strontium copper oxide antiferromagnet.

The strontium copper oxide compounds Sr_2CuO_3 and SrCuO_2 are one-dimensional (1-D) quantum antiferromagnets and thus believed to support spin-charge separation. To examine this phenomenon, some method that is sensitive to valence band excitations must be employed. Although x-ray scattering is a useful tool for probing bulk electronic structure, excitations of valence electrons yield a far weaker signal. In earlier work, the research team demonstrated that by tuning the incident x-ray energy near an absorption edge, a large enhancement of the valence band scattering could be observed, making possible detailed momentum-resolved studies of high- Z materials. In addition, because of the high brightness of third-generation synchrotrons such as the APS, scattering studies over the entire Brillouin zone were feasible.

Single-crystal samples of SrCuO_2 were grown and characterized for this study by established techniques and found to be

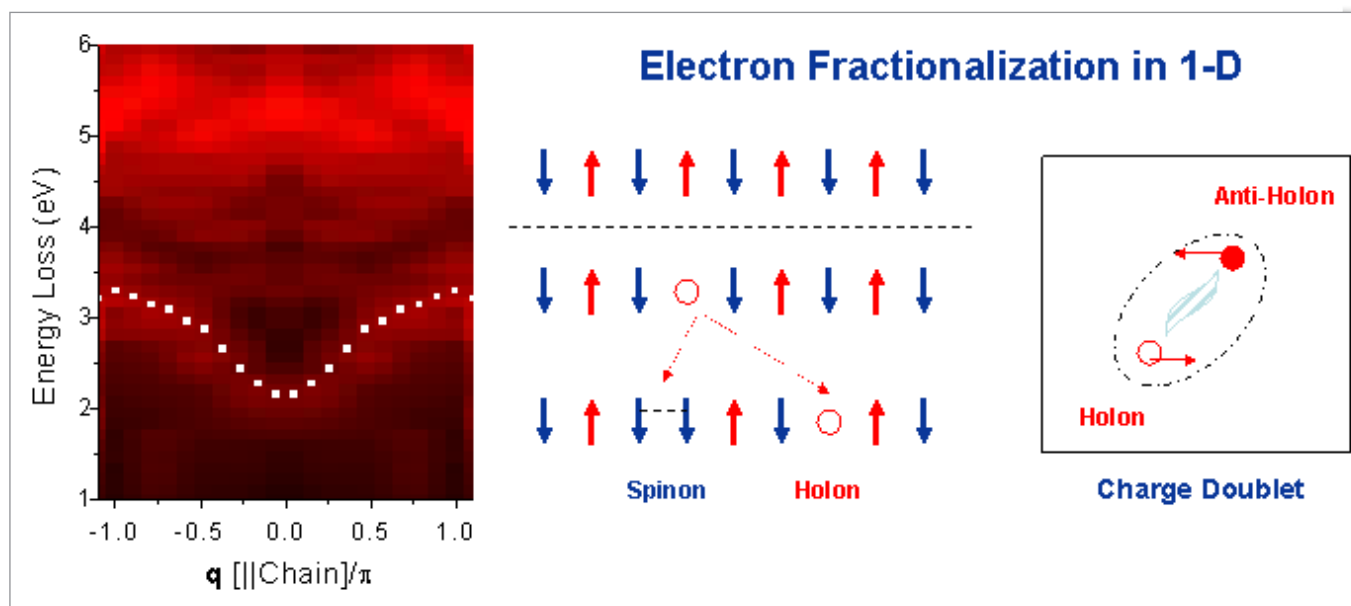


Fig. 1. Left: Dispersion plot of experimental inelastic x-ray scattering features as a function of q (red indicates high spectral intensity). Right: A cartoon view of electron fractionalization in 1-D. X-ray scattering couples to the charge part of the excitations and traces out holon excitation (holon-antiholon) spectrum. The necklace feature in the left figure corresponds to the holon-antiholon spectrum.

1-D spin chain materials at room temperature. The inelastic x-ray scattering data were obtained at the CMC-CAT beamline 9-ID and BESSRC/XOR beamline 12-ID at the APS. The incident beam energy was selected to be near the copper K edge at 8.997 keV to produce resonant scattering. The scattered beam was passed through a germanium spectrometer and measured with a solid-state detector. The overall energy resolution for the experiment was 350 meV. Scans over a range of q values were obtained by rotating the spectrometer about the scattering point on the sample. Data were also obtained for scans in energy through the Cu K edge.

Two features are seen in the inelastic x-ray scattering spectra as a function of q . One of these is approximately fixed at about 5.6 eV. The other is a lower-energy excitation, which can be interpreted as a particle-hole excitation across the Mott gap in the cuprate spin chain. In particular, the dispersion of this feature parallels the dispersion of the Mott gap itself. Moreover, the q -dependence in this 1-D material is stronger than that seen in previous measurements of two-dimensional materials, which is expected for spin-charge separation. A comparison with numerical studies also shows good agreement with holon formation in a half-filled spin-1/2 Hubbard model with charge fluctuations. Considered together, these observations are consistent with the observation of spin-charge separation and the formation of holons and antiholons in this cuprate (Fig. 1).

The data in the present experiment are, by their nature, sensitive primarily to the charge (holon) portion of the excitation. Single spin excitations are much weaker and would appear at a much lower energy than observable in this work. Future efforts, perhaps feasible at high-brightness facilities, such as

the Inelastic X-ray Scattering sector 30 at the APS, may allow much higher-resolution experiments that can capture the full range of spin-charge behavior in these interesting materials. ○

References

- [1] M.Z. Hasan^{1,2}, Y-D. Chuang³, Y. Li¹, P. Montano⁴, M. Beno⁴, Z. Hussain³, H. Eisaki¹⁵, S. Uchida⁶, T. Gog⁷, and D.M. Casa⁷, "Direct Spectroscopic Evidence of Holons in a Quantum Antiferromagnetic Spin-1/2 Chain," *Intl. J. of Mod. Phys. B* **17**(18, 19, 20), 3479-3483 (2003).
- [2] M.Z. Hasan, P.A. Montano, E.D. Isaacs, Z.-X. Shen, H. Eisaki, S.K. Sinha, Z. Islam, N. Motoyama, and S. Uchida, "Momentum-Resolved Charge Excitations in a Prototype One-Dimensional Mott Insulator," *Phys. Rev. Lett.* **88**, 177403 (2002).

See: Reference [1] above is the source of this article.

Author affiliations: ¹Princeton University, ²Princeton Materials Institute, ³Advanced Light Source, ⁴Argonne National Laboratory, ⁵National Center for Advanced Industrial Science and Technology (Tsukuba, Japan), ⁶University of Tokyo, ⁷CMC-CAT

This work was partially supported by National Science Foundation grant DMR-0213706. Use of the Advanced Photon Source was supported by the U.S. Department of Energy, Office of Science, Office of Basic Energy Sciences, under Contract No. W-31-109-Eng-38.

X-RAY SCATTERING REVEALS UNUSUAL GROWTH OF LEAD ON SILICON

Most thin films grow on substrates in only three ways: layer by layer, formation of atomic islands, or layers followed by islands. The particular growth mode that a given material will follow crucially depends on the relative magnitudes of the surface energy of the film versus the interfacial energy of the film on the substrate. Recently, a team of researchers from the University of Illinois, Academia Sinica in Taiwan, Georgia Institute of Technology, and the City University of Hong Kong has discovered a remarkable anomaly. By means of real-time x-ray scattering measurements, the researchers found that lead films grown on silicon adopt a completely novel pattern of growth.

Earlier studies of lead films on silicon with scanning tunneling microscopy and electron diffraction revealed hints that certain island heights above the substrate were preferred over others. These “magic” dimensions suggest that quantum size effects play a strong role in the formation of the films. Yet, the magic numbers do not seem to bear any relation to characteristic dimensions or length scales of the films themselves. In order to unravel this puzzle, the researchers also performed first-principles density functional calculations to understand their experimental results.

Real-time x-ray scattering measurements of the film structure were obtained with a growth chamber placed at the UNICAT beamline 33-ID at the APS. Lead vapor from an effusion cell was deposited at a rate of 0.0044 monolayers per second onto silicon substrates prepared to expose the (111)-7X7 surface. A CCD camera captured the scattered 26.05-keV x-rays from the APS undulator beam (Fig. 1) in order to measure reflectivity and truncation rod scattering at regular intervals. Film growth was monitored *in situ* with a vibrating quartz thickness gauge and the temperature of the sample was monitored with a thermocouple.

Truncation rod profiles obtained from the CCD images give a detailed picture of the film evolution during growth. From the interference fringes, information about island height and film thickness is deduced. At first, there is an increase in the intensity of the silicon surface diffraction, indicating that a lead wetting layer is forming, commensurate with the underlying substrate lattice. After a thickness of about 1.1 monolayer, the silicon diffraction intensity decreases, followed by a rise in lead intensity and island formation at a deposition of 1.5 monolayer. At this stage, the islands begin growing up to a height of 5 monolayers above the wetting layer (a net island height of 6 monolayers). Then, in an unusual departure from typical growth modes, the islands remain locked at this height but begin growing horizontally until all of the islands have filled in to form a single 6-monolayer film. Now the growth switches completely from island growth to layer-by-layer growth for the rest of the film's evolution.

Two characteristic thicknesses emerge from this analysis: the 1-monolayer wetting layer, which gives way to island for-

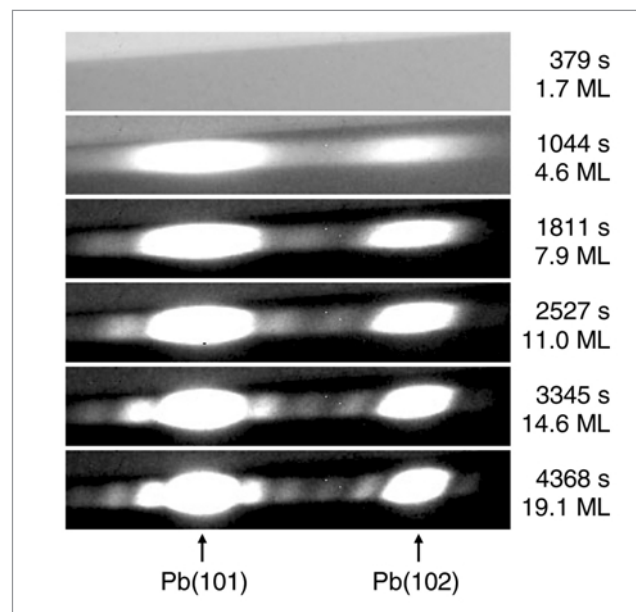


Fig. 1. X-ray diffraction images taken with a CCD camera during growth of Pb films on Si(111). The interference fringes yield information about island height and layer thickness.

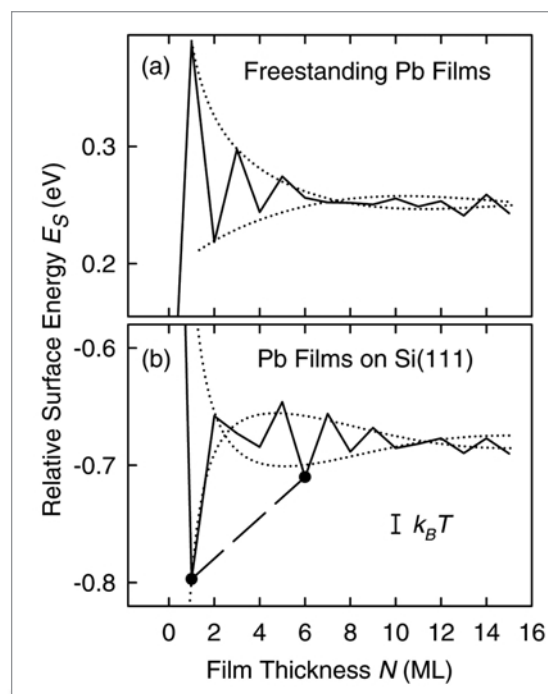


Fig. 2. First-principles calculations of (a) a free-standing Pb film and (b) Pb film on silicon substrate. The altered Friedel oscillations in (b) give rise to energy minima, which account for the magic island height and wetting layer.

mation, and the 6-monolayer magic island height. To make sense of these critical thicknesses, the researchers performed first-principles calculations of the relative surface energy per surface atom of the films (Fig. 2). For free-standing lead films, the energy follows a typical damped Friedel oscillation pattern with a period of 1.8 monolayer. When the calculation is done for lead atoms on a silicon substrate, however, the altered boundary condition produces a phase shift in the envelope function, resulting in deep minima at 1 monolayer and 6 monolayers.

The absolute energy minimum at 1 monolayer explains the wetting layer, while the minimum at 6 monolayers accounts for the magic island height. For coverages between these two values, the system would be expected to phase separate into a linear combination of the two, in excellent agreement with the behavior observed in the island formation. As shown by this work, taking into the consideration the global energy picture and not just the local energy landscape is essential in understanding the complete story of thin-film growth. ○

See: H. Hong¹, C.-M. Wei^{2,3}, M.Y. Chou³, Z. Wu¹, L. Basile¹, H. Chen⁶, M. Holt¹, and T.-C. Chiang¹, *Phys. Rev. Lett.* **90** (7), 076104-1 to 076104-4 (21 February 2003).

Author affiliations: ¹University of Illinois at Urbana-Champaign, ²Academia Sinica, ³Georgia Institute of Technology, ⁴City University of Hong Kong

This work was supported by the U.S. Department of Energy (Grants No. DEFG02-91ER45439 and No. DEFG02-97ER45632), the R.O.C. National Science Council (Grant No. 90-2112-M-001-062), the U.S. National Science Foundation (Grants No. DMR-02-03003 and No. SBE-01-23532), and the Petroleum Research Fund administered by the American Chemical Society. The UNI-CAT facility at the APS is supported by the University of Illinois Frederick Seitz Materials Research Laboratory (U.S. Department of Energy and the State of Illinois-IBHE-HECA), the Oak Ridge National Laboratory (U.S. Department of Energy under contract with Lockheed Martin Energy Research), the National Institute of Standards and Technology (U.S. Department of Commerce), and UOP LLC. The APS is supported by the U.S. Department of Energy (Grant No. W-31-109-Eng-38).

REVEALING THE NATURE OF INHOMOGENEOUS MAGNETIC STATES IN ARTIFICIAL FERRIMAGNETS



Artificial magnetic layered structures are widely used for applications in information storage (*i.e.*, magnetic memory). Current devices use homogeneous magnetic states, in which the layers' magnetization aligns parallel or antiparallel to an applied magnetic field. Parallel or antiparallel relative alignment of alternate layers results in significantly different electrical resistance, which makes the 0's and 1's of a binary logic base for storage and computation. Inhomogeneous magnetic states, in which the layers' magnetization can be made to orient at a variety of angles with respect to the applied field direction, could be used as a basis for a more complex but efficient logic scheme. The intermediate, inhomogeneous magnetic states also exhibit varying degrees of electrical resistance, which could provide the necessary signatures for higher speed storage and computation.

For years, science has tried to experimentally resolve the mechanism of nucleation of magnetic inhomogeneous states in artificial multilayers. By using grazing incidence x-ray magnetic circular dichroism (XMCD) at the XOR beamline 4-ID at the APS, experimenters from Argonne National Laboratory have successfully measured the low-field surface nucleation and evolution of the inhomogeneous magnetic state in strongly coupled Fe/Gd ferrimagnetic multilayers. The results of their research help explain the effect of surface termination upon nucleation of inhomogeneous magnetic states in magnetic multilayers.

The studies show that at nucleation, the magnetic surface state extends tens of interatomic distances into the bulk (approximately 200 Å) — a direct consequence of the strong antiferromagnetic interlayer coupling between the Fe (35 Å) and Gd (50 Å) layers. In this state, the magnetization deviates from the applied field direction in the near-surface region while

it remains field-aligned in the bulk. Tuning the sample temperature to near the compensation temperature, T_0 (at which the sublattice magnetizations are equal but opposite) causes the inhomogeneous state to penetrate throughout the bulk. Homogeneous magnetic states occur far below and above T_0 . Surface termination has a dramatic effect on the nature of the inhomogeneous state.

Before the work at APS, several techniques have been used to gather experimental evidence for a magnetic inhomogeneous state. The work at the APS is unique in that researchers took direct, real-space measurements of the low-field nucleation of an inhomogeneous magnetic state near the surface of an Fe-terminated ferrimagnetic multilayer.

For several years, it has been predicted that a phase transition into an inhomogeneous magnetic state would nucleate at the surface of a strongly coupled artificial ferromagnetic multilayer, if the multilayer was terminated by the minority magnetic component. In this "surface-twisted" phase, the magnetization deviates from the applied field direction near the surface, while the bulk remains field-aligned. Unfortunately, probing surface and bulk states in the same measurement has not been possible, making experimental detection of this inhomogeneous phase difficult. The challenge is to observe both the existence of a surface-twisted phase and the absence of a bulk twist.

This challenge was overcome through the use of the brilliant x-ray beams from the APS, which enable the collection of direct, real-space data on the near-surface and bulk magnetic states in the same measurement. This was achieved by exploiting the penetration depth tunability of the x-rays at grazing- and larger-incidence angles to alternately probe the surface and bulk magnetic states.

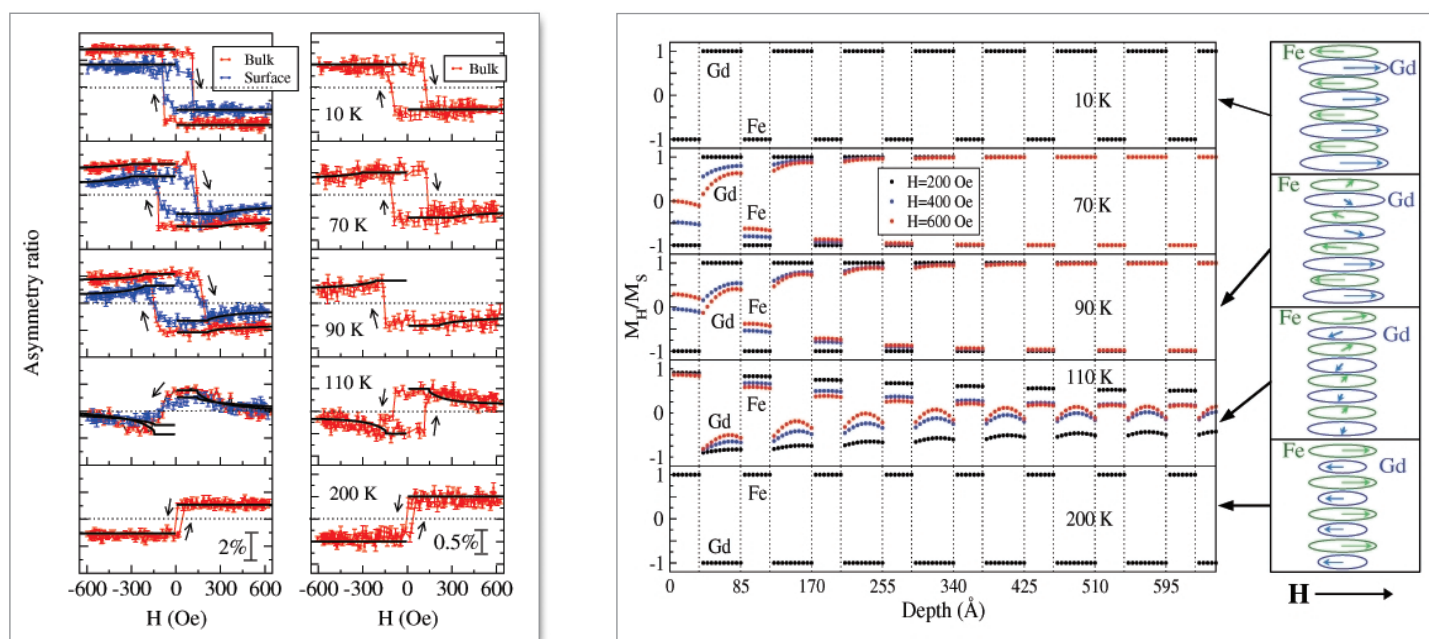


Fig. 1. Left panel: Gd (left) and Fe (right) hysteresis loops (points). Surface loops are scaled down for clarity. Right panel: Theoretical calculations of magnetization depth profiles, shown for half of the multilayer structure (other half is mirror symmetric). Profiles are normalized to saturation magnetization at each temperature. The schematic diagram (far right) represents the magnetization in the upper four bilayers (intralayer averaged) at $H = 600$ Oe. Calculated hysteresis loops are given by the solid lines superimposed on the data points of the left panel. "Flat" loops correspond to homogeneous magnetic states, while "tilted" loops indicate deviations of the magnetization from the applied field direction.

The unique experimental setup enabled the researchers to simultaneously measure specular reflectivity and XMCD in fluorescence geometry. Element-specific hysteresis loops were then measured at the resonant energies for which the magnetic contrast is the largest by reversing the x-ray helicity at each applied field value and measuring the asymmetry ratio *i.e.*, the difference in the absorption of opposite helicities of circularly polarized x-rays divided by its sum. To accurately determine the x-ray incidence angle, the specularly reflected signal was used. Despite constraints set by a Nb capping layer, researchers were able to retrieve surface-enhanced magnetic information from Gd layers. These constraints, however, led to reduced surface sensitivity at the Fe resonance. A fit to the specular reflectivity data (modified to include roughness) confirmed the nominal structural parameters of the multilayer.

Comparing the experimental results with theoretical calculations of the static magnetization profile validated the accuracy of this approach. Researchers found that the calculations were in good agreement with the experimental results and supported the conclusion of the extent of the penetration depth at nucle-

ation. By contrast, the results of previous attempts to determine the penetration depth at nucleation indicated that it was several thousand angstroms—a significant difference. The results at the APS are the first to directly confirm the long-ago predicted inhomogeneous magnetic phase in the strongly coupled model system. The method also promises to open new doors for distinguishing surface from bulk states in other inhomogeneous magnetic systems. ○

See: D. Haskel, G. Srajer, Y. Choi, D.R. Lee, J.C. Lang, J. Meersschaet, J.S. Jiang, and S.D. Bader, "Nature of inhomogeneous magnetic state in artificial Fe/Gd ferrimagnetic multilayers," *Phys. Rev. B* **67**, 180406-1 (R) to 180406-4 (R) (2003).

Author affiliations: Argonne National Laboratory

J.M. was supported by the Belgian Science Foundation (F.W.O.-Vlaanderen). Use of the Advanced Photon Source was supported by the U.S. Department of Energy, Office of Science, Office of Basic Energy Sciences, under Contract No. W-31-109-Eng-38.

